World Electric Vehicle Journal

MDPI

Article

Research on Filtering Algorithm of Vehicle Dynamic Weighing Signal

Lingcong Xiong *, **Tieyi Zhang, Anlu Yuan and Zhipeng Zhang**

School of Mechanical Engineering, Guangxi University, Nanning 530004, China; zty200@gxu.edu.cn (T.Z.); 2211391070@st.gxu.edu.cn (A.Y.); 2211391078@st.gxu.edu.cn (Z.Z.)

* Correspondence: 2211391063@st.gxu.edu.cn

Abstract: This study analyzes the advantages and disadvantages of filtering algorithms for dynamic weighing signals. Highway road surface has road surface unevenness and other influencing factors. The body vibration of the vehicle driving process produces a certain amount of interference signals collected by the load cell to form noise signals. In addition, piezoelectric sensors and amplification circuits introduce a large amount of electrical noise. These noise signals are non-smooth, nonlinear, and have other characteristics. We study the filtering effects of moving average (MA), wavelet transform (WT), and variational mode decomposition (VMD) filtering algorithms on axle weight signals and evaluate the performance of the filtering algorithms through the Root Mean Square Error (RMSE), signal-to-noise ratio (SNR), and Normalized Correlation Coefficient (NCC). The comprehensive analysis shows that the variational modal decomposition filtering algorithm is more advantageous for axial weight signal processing. The design of the axle weight signal noise filtering algorithm is of great significance for improving the accuracy of the overall dynamic weighing system of the vehicle.

Keywords: dynamic weighing; filtering algorithm; noise signals; axle weight signal; moving average; wavelet transform; variational modal decomposition

Citation: Xiong, L.; Zhang, T.; Yuan, A.; Zhang, Z. Research on Filtering Algorithm of Vehicle Dynamic Weighing Signal. *World Electr. Veh. J.* **2024**, *15*, 254. https://doi.org/10.3390/wevj15060254

Academic Editors: Quan Yuan and Xiaoyuan Fu

Received: 9 May 2024
Revised: 6 June 2024
Accepted: 7 June 2024
Published: 12 June 2024

1. Introduction

The development of dynamic weighing technology has evolved from traditional methods to modern algorithms. Initially, simple sensors and analog filters were used for weight measurement and signal processing, but these methods struggled to cope with noise and interference in complex environments. With the rise in digital signal processing technology, digital filtering techniques replaced traditional analog filters, providing higher accuracy and reliability for the system [1]. Subsequently, the introduction of technologies like wavelet transform made signal analysis more flexible and efficient, enabling accurate capture of dynamic characteristics and periodic changes in the signal [2]. In recent years, the application of artificial intelligence technologies such as machine learning and deep learning has brought new opportunities for dynamic weighing, allowing for the automatic extraction of signal features and patterns by learning from large amounts of data, achieving high-precision weight measurement, and noise suppression [3–5].

With the development of modern society, dynamic weighing technology has been widely used in various fields. The dynamic weighing system is widely used in logistics, transportation, medical, automobile, and industrial fields, providing an effective means of weight monitoring for various industries [6–11]. In these applications, the signal generated by the dynamic weighing system is often affected by various environmental factors, including vibration, noise, and other interference factors. These interference signals may lead to inaccurate weighing results, which affects the performance and stability of the system.

Therefore, the study of dynamic weighing signal filtering algorithms has become an important topic in the current scientific and technological research field. By using a reasonable signal filtering method, we can effectively improve the measurement accuracy of the dynamic weighing system, reduce system error, and enhance the reliability and stability of the system. The purpose of this thesis is to explore and study the filtering algorithm for dynamic weighing signals and to provide strong support for the further development and application of dynamic weighing technology.

There are two methods of signal filtering: software filtering and hardware filtering. Hardware filtering is mainly filtered through a hardware circuit composed of capacitors resistors and operational amplifiers, which is low in cost and easy to implement, but its accuracy is not high, and its function is limited [12]. The software filter mainly uses the existing or improved filtering algorithm to process the original signal, which has good controllability and filtering effects. The research shows that signal noise is usually a specific frequency band and high-frequency noise [13,14]. In recent years, the filtering methods used in the literature related to dynamic weighing mainly include the Kalman filter (KF), MA [15,16], adaptive filter, median filter, WT [17,18], mode decomposition [19–21], and other filtering algorithms. Kalman filter is a recursive filtering algorithm that is widely used to estimate the state of dynamic systems. In the field of dynamic weighing, Kalman filters can be used to reduce the errors caused by measurement noise and environmental interference. Research [22] proposes a new Kalman filter, called the maximum correlation entropy Kalman filter (MCKF), which adopts the robust maximum correlation entropy criterion (MCC) as the optimal criterion instead of MMSE. The effectiveness and robustness of the filter are demonstrated by an example. In a study [6], the Kalman filter was used to update the real-time weight estimation, which effectively improved the weighing accuracy of ships. MA is a simple and practical filtering algorithm with strong signal smoothing ability. Based on the vibration characteristics of the vehicle and scale, the mathematical model of the WIM signal is established by moving average filtering and the B-spline least square method in research [23], and the vibration interference of low-frequency dynamic load is effectively eliminated. The adaptive filter adjusts the filtering parameters according to the real-time measurement data to adapt to different environmental conditions. This method can improve the adaptability of the system to the dynamic environment change. Median filtering is a nonlinear filtering method that suppresses outliers by calculating the median of the data in the window. In dynamic weighing, median filtering can effectively remove abnormal data caused by burst interference. WT is a time-frequency analysis method that realizes signal filtering by eliminating noise signals by threshold; it is widely used in various fields. In this study [24], strain data collected by FBG sensors embedded in road sections were used to evaluate the performance of discrete wavelet transform (DWT) in de-noising FBG signals. The results show that the FBG signal can be successfully de-noised, and the low-amplitude strain can fully emerge without losing any valuable data. The mode decomposition method is a data-driven adaptive signal decomposition filtering method, and its frequency band is not fixed. Empirical mode decomposition (EMD) and its improved methods, such as ensemble empirical mode decomposition and complementary ensemble empirical mode decomposition, are EMD-like methods. There is also the VMD method; VMD decomposition is different from EMD and is an adaptive, completely non-recursive mode variation and signal processing method. In a study [25], the difference between the sum of IMFs obtained from the original signal and VMD was used to realize the fuzzy optimization of the preset scale K value and extract the main features of the signal. This method has the maximum output SNR and the minimum mean square error and realizes the fuzzy optimization of K. The effectiveness of this method in filtering pipeline leakage signals is verified by experiments. Research [26] used acceleration sensors to acquire vehicle vibration to assist ensemble empirical mode decomposition and improve wavelet threshold noise reduction algorithm to improve the accuracy and accuracy of system measurement. Research [27] proposed a hyper-local non-model predictive algorithm, which can be applicable to complex or unknown systems, enabling rapid response and processing of input–output data, thus achieving efficient real-time control. It demonstrates excellent performance in control and prediction but mainly focuses on real-time control and prediction, paying less attention to the frequency domain characteristics of signals. Specialized filtering algorithms such as VMD would be beneficial for addressing this aspect.

The core problem of this study is to select more appropriate signal filtering algorithms in vehicle dynamic weighing systems to improve the accuracy and reliability of weighing data. Reducing the noise and interference in the signal and improving the performance of the dynamic weighing system will not only help vehicle overload monitoring but also provide reliable data support for vehicle research, traffic management, road safety, logistics, and transportation. For this purpose, signal analysis, filtering algorithm design, and comparative validation are used in this study. The frequency characteristics and noise characteristics of the vehicle dynamic weighing signal are analyzed, and suitable filtering algorithms are designed and selected, including moving average filtering, wavelet transform, and variational mode decomposition filtering. Finally, the performance of the filtering algorithms is compared by filtering the actual axle weight signal.

2. Dynamic Weighing Signal Analysis

To perform the characterization of the actual axle weight signals, a dynamic weighing system based on a PVDF piezoelectric film sensor was used in this study to collect the axle weight information. As shown in Figure 1, the experimentally collected axle weight data come from a common two-axle vehicle. When the axle of the vehicle passes through the PVDF piezoelectric thin film sensor, the system can acquire the specific raw signal.

Figure 1. Experimental diagram of axle load signal acquisition.

When the two-axle vehicle traveled through the dynamic load sensor, the original piezoelectric signal collected is shown in Figure 2 (the sampling interval is 0.0002 s, which means the sampling frequency is 5000 Hz). Figure 2a shows the original signal waveform when a two-axle vehicle passes the sensor. There is a slight asymmetric distortion in the waveform, and there is a wave valley at the end of the signal pulse decline, which is caused by the sensor deformation bending and rebounding. Figure 2b shows the original signal waveform when no vehicle passes through the sensor. It can be seen that there is a noise signal, and the amplitude of the noise signal is between −0.002 and 0.002.

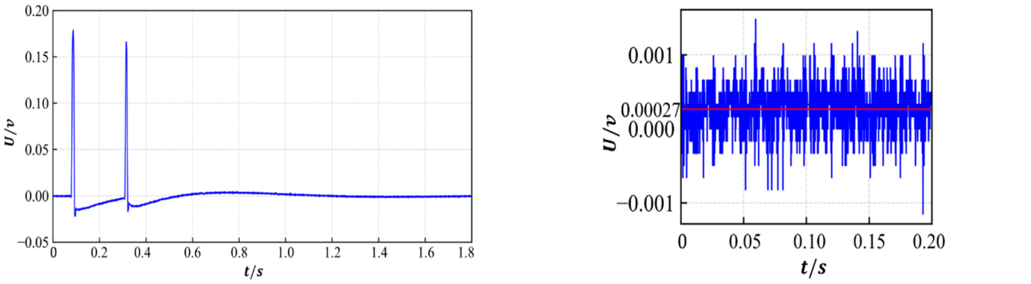

(**a**) Vehicle passing signal waves. (**b**) Without vehicular traffic signal waves.

Figure 2. Raw load piezoelectric signal.

After the Fast Fourier transform (FFT) of the acquired signal, the amplitude–frequency diagram shown in Figure 3 is obtained, and the signal is mainly concentrated in the low-frequency part, in the range of 0 to 250 Hz, from the low frequency to the high frequency, the amplitude is constantly decaying, in which the amplitude is the largest in the lowest frequency part, as shown in Figure 3a, and the subsequent decaying part belongs to the interference signal, which is generated by the vibration of the tire suspension system and the vehicle driving, with the frequency of fifty to several hundred Hz [23]. In Figure 3b, in the frequency range of 250 to 2500 Hz, it can be seen that there is a portion of high-frequency noise; the 200 to 1800 Hz high-frequency noise accounted for a relatively small amount of high-frequency noise, and high-frequency noise is mainly concentrated in the 2000 to 2500 Hz.

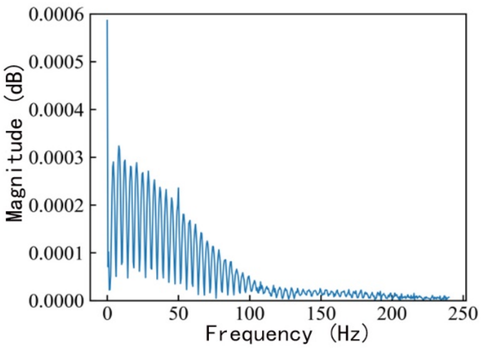

(**a**) 0~250 Hz

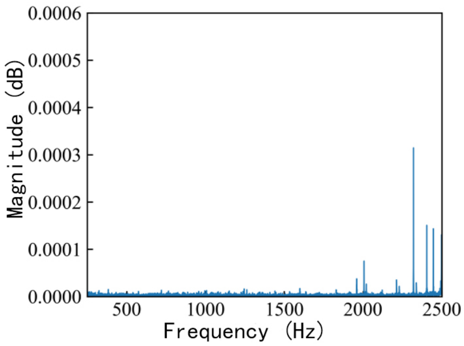

(**b**) 250~2500 Hz

Figure 3. Dynamic weighing signal amplitude and frequency diagram.

3. Dynamic Weighing Signal Filtering Algorithm Analysis

3.1. Moving Average Filtering

For a segment of discrete input signal $x(n)$, the MA filters first determine a sliding window of length N, average the next sampled value with the temporarily stored $N-1$ values to obtain the effective value, and at the same time update the value at the forefront of the window to that effective value and slides forward. It has good suppression of periodic interference and good suppression of random noise. MA filters are simple to implement and are usually the first method to try.

The most critical parameter of the MA filter is the selection of the sliding window size, which in the time domain is the length of the convolution kernel when using a rectangular function as the convolution kernel. The output of the MA filter is:

$$y(n) = \frac{1}{N}\sum_{k=1}^{N} x\ (n+k) \tag{1}$$

where $y(n)$ is the filter output, and N is the window length. The Fourier transform of Equation (1) yields the frequency response as:

$$Y\left(e^{j*2\pi f}\right) = \frac{1}{2m+1}\left\{1+2\sum_{k=1}^{m} cos(k*2\pi f)\right\} \tag{2}$$

where m is half the size of the filter window (excluding the center point), i.e., $N = 2m + 1$.

The form of $Y(n)$ is similar to that of the Singer function, which is characterized by slow roll-off of the transition band and insignificant rejection of the blocking band.

MA filtering is usually the preferred filtering algorithm to try in signal processing due to its simplicity and efficiency. The relationship between the window length and the cutoff frequency of MA can be expressed as:

$$N = \frac{0.443 * f_s}{f_{co}} \tag{3}$$

where f_s is the sampling frequency, and f_{co} is the cutoff frequency. In the vehicle dynamic weighing system, the sampling rate is set to 5 kHz, and according to the signal frequency distribution in Figure 3, the cutoff frequency is selected as 100 Hz, and N is calculated to be 22.

3.2. Wavelet Transform Filtering

WT is mainly used for signal processing and analysis in both time and frequency domains. Wavelets are mathematical functions of short duration that can be expanded and translated along a given signal, enabling the analysis of signals at different scales. They are suitable for detecting parts of a signal that appear in short duration and change rapidly. WT filtering algorithms are widely used in one-dimensional signal processing [28,29].

Wavelets are signals with limited energy, ripples in one section, and fast decay on both sides. WT is different from the Fourier transform based on infinite length signals for transformation, which uses finite, decaying signals for base transform. The formula for wavelet transform is:

$$\vec{\psi}_{(a,b)}(x) = \frac{1}{\sqrt{a}}\psi\left(\frac{x-b}{a}\right) \tag{4}$$

where a is the scale parameter, controlling the stretching of the wavelet function in both time and frequency domains; b is the translation parameter, controlling the shifting of the wavelet function along the time axis. For the acquired load signal $f(x)$, the WT is:

$$W_j(a,b) = \int_R f(x)\vec{\psi}_{(a,b)}(x)dx = \frac{1}{\sqrt{|a|}}\int_R f(x)\vec{\psi}\left(\frac{x-b}{a}\right)dx \tag{5}$$

The discrete wavelet transform (DWT) is a discretization of the scale and translation of the fundamental wavelet, and the one-dimensional DWT is

$$\begin{cases} a_{j,k} = \int f(t)\psi^*_{j,k}(t)dt \\ f(t) = \sum_k \sum_j a_{j,k}\psi_{j,k}(t) \\ \psi_{j,k}(t) = 2^{\frac{j}{2}}\psi(2^j t - k) \end{cases} \tag{6}$$

where j is the scale parameter, controlling the stretching of the wavelet function and determining its frequency; k is the position parameter, determining the position of the wavelet function along the time axis.

After a DWT, the signal S is decomposed into:

$$S = A_1 + D \tag{7}$$

where A_1 is the relatively low-frequency approximation component, and D is the relatively high-frequency detail component.

Due to the orthogonalization constraints, the component obtained after each decomposition is half of the original signal length, and the decomposition is performed again for low frequencies to obtain A_2 and D_2, and so on, i.e., multi-level discrete wavelet decomposition (Figure 4). The time series signal is divided into multiple sub-sequences of low and high frequencies, step by step, to extract multi-level time-frequency features:

$$S = A_n + \sum_{i=1}^{n} D_i \tag{8}$$

where n is the number of decomposition levels, and D_i is the detail component corresponding to each decomposition level.

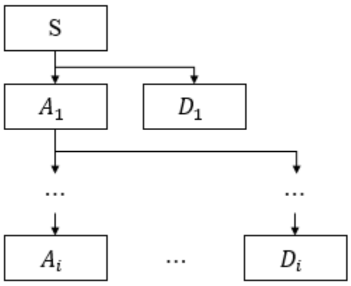

Figure 4. Multi-stage discrete wavelet transform diagram.

In the wavelet decomposition of the signal, the larger the number of layers of decomposition achieved, the more obvious the different characteristics of the noise and signal performance, the more conducive to the separation of the two, but the larger the number of layers of decomposition, the larger the distortion of the reconstructed signal will be, which, to a certain extent, leads to the deterioration of the filtering effect. According to the results of the FFT in Figure 2, the dynamic weighing effective signal is mainly concentrated below 100 Hz, while the adopted frequency F_s is 5 kHz, according to:

$$\frac{0.5 \times F_s}{2^N} = \frac{f_{max}}{2^N} \tag{9}$$

The signal is decomposed five times using multi-level wavelet decomposition to obtain the score band frequency of 0~39.06 Hz, 39.06~78.125 Hz, 78.125~312.5 Hz, 312.5~1250 Hz, 1250~2500 Hz; each band division is more in line with the characteristics of the signal, which is conducive to the analysis of the low-frequency part of the signal composition.

The filtering effect is achieved by wavelet thresholding before wavelet reconstruction. Wavelet thresholding noise reduction is divided into hard thresholding noise reduction and soft thresholding noise reduction. Hard threshold noise reduction is to compare the wavelet coefficients of multiple high-frequency components D_i with the threshold and keep the components unchanged if they are greater than or equal to the threshold; if they are smaller than the threshold, the components are directly set to zero. In soft-threshold noise reduction, each high-frequency component is compared to a threshold, and if it is greater than or equal to the threshold, the component is subtracted from the threshold; if it is less than the threshold, the component is directly set to zero. This strategy is used in multi-level wavelet decomposition for each component of each layer to filter out signals in specific frequency bands. Finally, wavelet reconstruction of the signal is performed, which is an inverse transformation of the wavelet decomposition. For the thresholded component combinations, the component lengths are not equal to the original signal lengths and cannot be reconstructed directly; the signal is reconstructed by choosing a suitable orthogonal mirror filter.

3.3. Variational Mode Decomposition Filtering

In recent years, scholars have applied the modal decomposition method to dynamic weighing signal processing [30,31]. EMD and other modal decomposition methods decompose the original signal into multiple Intrinsic Mode Functions (IMF) and a residual component. By zeroing specific frequency signals, the signal is synthesized to realize the filtering effect of the signal. In the literature [32], the complementary ensemble empirical mode decomposition (CEEMD) was used to separate the low-frequency interference in the real weighing signal, and the residual component was used as the input to train the GRU neural network, which improved the weighing accuracy. It can be seen that the modal decomposition method has some advantages in dealing with dynamic weighing signals where effectiveness and interference are mixed at low frequencies.

Due to the problems of endpoint effect and frequency aliasing in empirical modal decomposition, Dragomiretskiy et al. [33] proposed the VMD method, which is a non-recursive signal processing method that can decompose a time series signal into a series of frequency components with finite bandwidths by iteratively searching for the optimal solution of the variational modes, and can adaptively update the center frequencies and bandwidths of each component, avoiding the problems of endpoint effect and spurious components encountered in the iterative process. It can adaptively update the center frequency and bandwidth of each component, avoiding the endpoint effect and false component problems encountered in the iterative process, and it can effectively deal with nonlinear and non-smooth signals.

The VMD algorithm assumes that the original signal $x(t)$ consists of a superposition of K modal functions with center frequency w_k, where IMF is defined as:

$$u_k(t) = A_k(t)cos(\phi_k(t)) \tag{10}$$

The above equation represents the harmonic signal of the kth mode $u_k(t)$ with amplitude $A_k(t)$ and instantaneous phase $\phi_k(t)$ and constrains the IMF to be a finite-bandwidth signal with a center frequency and the minimum sum of modal bandwidths to construct the constrained variational model:

$$\min_{\{u_k\},\{\omega_k\}} \left\{ \sum_k \| \partial_t \left[\left(\delta(t) + \frac{j}{\pi t} \right) * u_k(t) \right] e^{-j\omega_k t} \|_2^2 \right\} \tag{11}$$

$$\sum_k u_k = f \tag{12}$$

In Equation (10), u_k is the function of each mode, and ω_k is the center frequency of each mode; $\left(\delta(t) + \frac{j}{\pi t}\right) * u_k(t)$ is the Hilbert-transformed resolved signal of the modes; $e^{(-j\omega kt)}$ makes the modal function's spectral modulation to the corresponding fundamental band; and finally, the signal is modulated by Gaussian smoothing. Equation (11) is the constraint that the sum of the modes is equal to the original signal.

For solving the above variational problem, in the literature [33], the constrained problem is transformed into an unconstrained variational problem by using quadratic penalty terms and the Lagrange multiplier method:

$$\begin{aligned} \mathcal{L}(\{u_k\}, \omega_k, \lambda) := \alpha \sum_k \| \partial_t \left[\left(\delta(t) + \frac{j}{\pi t} \right) * u_k(t) \right] e^{-j\omega_k t} \|_2^2 \\ + \| f(t) - \sum_k u_k(t) \|_2^2 + \left\langle \lambda(t), f(t) - \sum_k u_k(t) \right\rangle \end{aligned} \tag{13}$$

where α is the penalty parameter, and λ is the Lagrange multiplier. The individual modes are then updated using the alternating multiplier method:

$$\hat{u}_k^{n+1}(\omega) = \frac{\hat{f}(\omega) - \sum_{i<k} \hat{u}_i^{n+1}(\omega) - \sum_{i>k} \hat{u}_i^n(\omega) + \frac{\hat{\lambda}^n(\omega)}{2}}{1 + 2\alpha\left(\omega - \omega_k^n\right)^2} \tag{14}$$

The center frequency is updated as follows:

$$\omega_k^{n+1} = \frac{\int_0^\infty \omega \left| \hat{u}_k^{n+1}(\omega) \right|^2 d\omega}{\int_0^\infty \left| \hat{u}_k^{n+1}(\omega) \right|^2 d\omega} \tag{15}$$

Lagrange multipliers λ are updated as follows:

$$\hat{\lambda}^{n+1}(\omega) \leftarrow \hat{\lambda}^{n}(\omega) + \tau\left(\hat{f}(\omega) - \sum_{k} \hat{u}_{k}^{n+1}(\omega)\right) \quad (16)$$

Each parameter is repeatedly updated until the iteration stop condition is satisfied:

$$\frac{\sum_k \| \hat{u}_k^{n+1} - \hat{u}_k^{n} \|_2^2}{\| \hat{u}_k^{n} \|_2^2} < \epsilon \quad (17)$$

where ϵ is used as the threshold for the stopping criterion, and its value is set to 10^{-7} here.

The flowchart of the algorithm to summarize the VMD is shown in Figure 5:

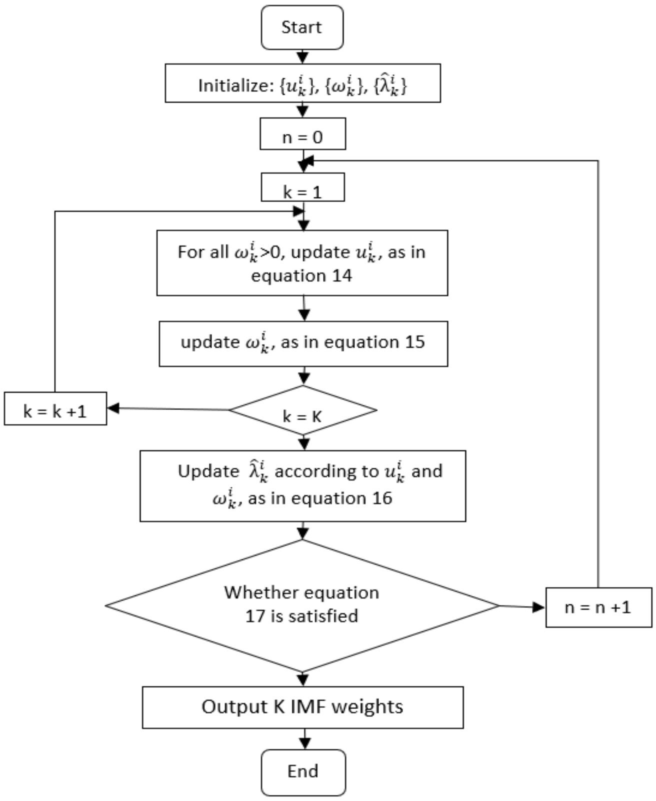

Figure 5. VMD algorithm flow chart.

When using the VMD algorithm for signal decomposition, some parameters need to be set. The decomposition result of the signal is related to the set parameters. The main parameters that need to be set for the VMD algorithm are the penalty factor, the balancing parameter for representing the data fidelity constraints, the time step, the number of decomposition layers K, and the convergence tolerance, where all the parameters except K have corresponding empirical values.

The most important of these parameters is the number of modal components, K. If K is set smaller than the number of useful components in the signal to be decomposed, it will result in inadequate decomposition, leading to modal aliasing. If the set K value is larger than the number of useful components in the signal to be decomposed, it leads to the generation of some useless spurious components. Therefore, the determination of the K value is very important for VMD. The main method used to determine the number of modes is as follows:

(1) By analyzing the frequency components mainly contained in the signal data, this method is usually used when the signal composition is simple.
(2) Attempts are made one by one through the K value from small to large; as the K value increases, the data of each major frequency band can be distributed into different IMF components, and the K value is analyzed and determined by combining the decomposition results. The method is time-costly and requires much tedious, repetitive work in the presence of multiple sensor signals.
(3) The VMD decomposition parameters are determined using auxiliary algorithms, e.g., according to the principle of craggy maximum, the principle of energy difference, etc. [34], or optimization algorithms are used (e.g., genetic algorithms, etc.), which use the signal-to-noise ratio of the decomposed reconstructed signals as the optimization objective, to obtain the optimal K-value.

Similar to WT filtering, after completing the decomposition of the signal by VMD, the filtered signal needs to be restored by inverse transformation, but the decomposition of VMD is simpler compared to WT filtering, and it only needs to accumulate the decomposed valid signals to realize the filtering of the signal.

4. Performance Experiment of Filtering Algorithm

4.1. Filtering Effect Evaluation Index

Dynamic weighing signals will lead to some information loss in the filtering process. To compare the denoising effect of the MA filter, WT filter, and VMD filter, the indicators of good or bad filtering effect, Root Mean Square Error (RMSE), Standard Deviation (SD), and signal-to-noise ratio (SNR) are used to objectively evaluate the algorithm performance with the following formulas:

$$RMSE = \sqrt{\frac{1}{N}\sum_{n=1}^{N}[x(n) - y(n)]^2} \tag{18}$$

$$SD = \sqrt{\frac{\sum_{i=1}^{n}(x_i - \overline{x})^2}{N}} \tag{19}$$

$$SNR = 10log\left(\frac{\sum_{n=1}^{N} y^2(n)}{\sum_{n=1}^{N}[x(n) - y(n)]^2}\right) \tag{20}$$

where N represents the sample size, $x(n)$ denotes the actual noisy signal, $y(n)$ stands for the corresponding ideal noise-free signal to $x(n)$, and $\overline{x}$ denotes the signal mean. Among them, *RMSE* mainly focuses on the accuracy of the filtered signal compared to the original signal. A smaller *RMSE* indicates better signal recovery. *SD* mainly focuses on the smoothness and consistency of the signal. A smaller *SD* indicates less fluctuation in the filtered signal. *SNR* mainly focuses on the ratio of useful information to noise in the filtered signal. A higher *SNR* indicates a higher quality of the filtered signal.

In addition, by comparing the waveform characteristics of the load signal before and after noise reduction (such as signal peaks, peak-to-peak intervals, peak width, etc.) to determine whether the waveform characteristics before and after filtering are lost and whether the waveform signal has been improved, to ensure the consistency of the waveform characteristics before and after filtering.

4.2. Experimentation

Python is an open-source, free programming language. Anyone can freely download, install, and use it. Additionally, Python's license is an open-source license released by the Python Software Foundation. All three filtering algorithms are implemented using Python 3.10. The MA filtering algorithm is relatively simple and can be directly edited in programming software by creating files for algorithm editing. The WT filtering algorithm is designed and edited using Python's 'pywt' library. The VMD filtering algorithm is implemented by porting the VMD library from MATLAB to Python for algorithm design. The hardware environment consists of a laptop with a CPU i7-10750H and 8 GB of memory, tested on the Windows 10 operating system. According to the previous analysis, the key parameter of MA filtering is the sliding window length, and the window length is selected as 22; for WT filtering, 5-level wavelet decomposition is performed. For the VMD algorithm, due to the complexity of the frequency components of the load signal, it is not possible to determine the number of decomposition modes, and it is chosen to determine the number of modes K using a gradual increase in the number of decomposition layers, starting from K = 2. The other parameters are chosen as follows: bandwidth limitation of 2500 Hz, noise tolerance of 0.00006, initialization of the data distribution parameters as a normal distribution, and the control error and iteration accuracy of 1e−6. The results of its experiments are as follows in Table 1:

Table 1. The center frequency of different K value decomposition.

K	IMF_1	IMF_2	IMF_3	IMF_4	IMF_5	IMF_6	IMF_7
2	23.85	5717.77					
3	32.33	141.62	2009.99				
4	36.95	399.94	1157.44	1689.93			
5	12.23	54.79	5421.66	7656.02	23,954.95		
6	7.73	12.18	122.71	598.11	5252.21	14,500.50	
7	6.84	21.62	26.56	62.56	349.75	7292.42	13,198.54

As the number of modes K increases from 2 to 7, the low-frequency bands are divided with less and less granularity. This implies that more modes are utilized to describe the various frequency components of the signal. Such meticulous decomposition enables VMD to capture the signal's local characteristics and frequency distribution more accurately.

From the center frequencies of each IMF component in the above table, it can be seen that the low-frequency components are divided more granularly as the decomposition reaches the 5th, 6th, and 7th layers, whereas the high-frequency components are increased as the number of decomposition layers increases. According to the analysis of the signal frequency components in the previous section, the axial load signal is mainly concentrated below 100 Hz, so the number of decomposition layers K is selected as 6.

Under the decomposition of 6-layer VMD, each IMF component is shown in Figure 6. It can be observed that IMF_5 and IMF_6 exhibit small amplitude and significant fluctuations, indicating noise components. IMFs 1 to 4 display distinct bimodal waveform characteristics consistent with the original axle load signal. Therefore, only IMF_1 to IMF_4 are selected for signal reconstruction through summation.

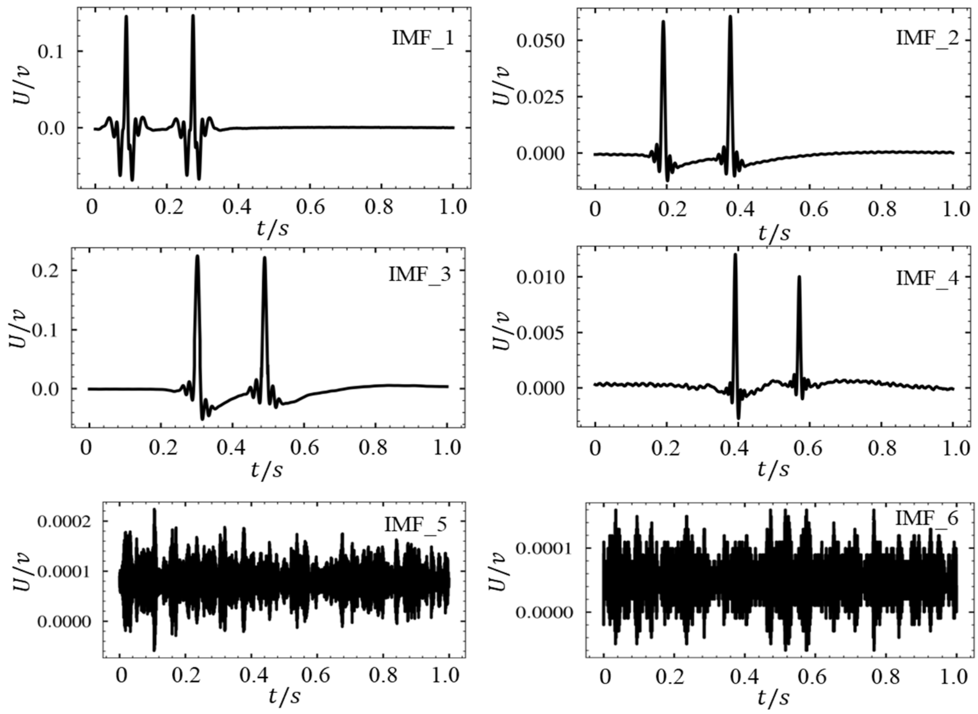

Figure 6. IMF components after VMD decomposition of 6 layers.

After selecting the appropriate parameters of the filtering algorithm, the results of the indexes after applying MA filtering, WT filtering, and VMD filtering to the noised ideal axial load signals are shown in Tables 2–4, respectively.

Table 2. MA filtered results.

Sensors	RMSE	SD	SNR
I	1.47×10^{-2}	1.53×10^{-2}	1.84
II	1.79×10^{-2}	2.08×10^{-2}	2.589

Table 3. WT filtering result.

Sensors	RMSE	SD	SNR
I	1.15×10^{-3}	1.81×10^{-2}	23.96
II	2.13×10^{-2}	2.39×10^{-2}	21.04

Table 4. VMD filtering results.

Sensors	RMSE	SD	SNR
I	7.69×10^{-4}	15.31×10^{-3}	27.14
II	1.24×10^{-3}	20.76×10^{-3}	24.74

After each filtering algorithm processes the sampled signal, the details of the waveform are shown in Figure 7. In the figure, SIG represents the original signal, DWT represents the signal after filtering using the wavelet transform algorithm, VMD represents the signal after filtering using the variational mode decomposition algorithm, and MA represents the signal after filtering using the moving average algorithm. The comparison of the processed signals shows that after the MA filtering process, the action signal becomes wider and shorter, and the degree of smoothing is higher after filtering; WT filtering and VMD filtering can better retain the waveform characteristics, and the curve of the original signal has a high degree of overlap. At the same time, the signal smoothness after the VMD filtering is higher than the WT filtering.

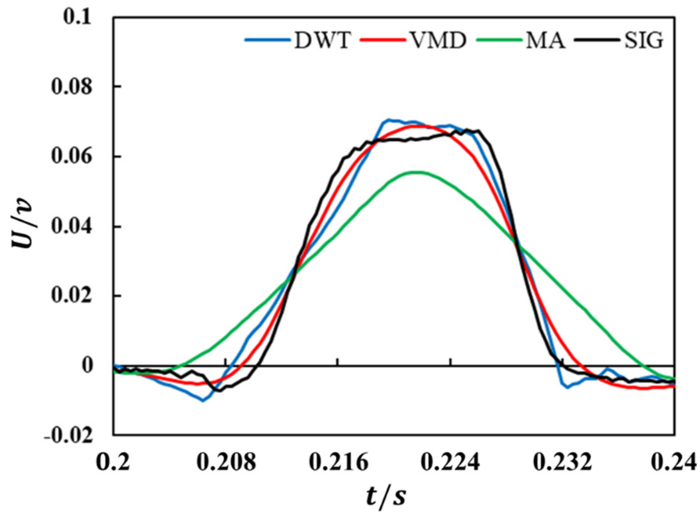

Figure 7. Comparison results of waveform details after filtering by each algorithm.

5. Conclusions

The main objective of this study was to develop and evaluate three filtering algorithms (moving average, wavelet transform, and variational mode decomposition) for processing axle weight signals in a vehicle dynamic weighing system. This was achieved by processing the collected raw axle load signals and comparing their filtering effects.

The moving average filtering algorithm has the advantages of simplicity, easy implementation, and low computational cost. The experimental results (Table 2) show that the RMSE values of the moving average filtering are 1.47×10^{-2} (Sensor I) and 1.79×10^{-2} (Sensor II), with SD values of 1.53×10^{-2} and 2.08×10^{-2}, respectively, and SNR values of 1.84 and 2.589, respectively. The processed signals become wider and shorter, and although they have greater smoothness, the loss of signal characteristics is significant.

Wavelet transform filtering can analyze signals at multiple scales and shows excellent removal of high-frequency noise. The experimental results (Table 3) show that the RMSE values of wavelet transform filtering are 1.15×10^{-3} (Sensor I) and 2.13×10^{-2} (Sensor II), with SD values of 1.81×10^{-2} and 2.39×10^{-2}, respectively, and SNR values of 23.96 and 21.04, respectively. The signals after filtering can better preserve waveform characteristics and have a high overlap with the original signal curve.

VMD filtering efficiently suppresses noise by decomposing the signal into several modal components. The experimental results (Table 4) show that the RMSE values of VMD filtering are 7.69×10^{-4} (Sensor I) and 1.24×10^{-3} (Sensor II), with SD values of 15.31×10^{-3} and 20.76×10^{-3}, respectively, and SNR values of 27.14 and 24.74, respectively. After filtering, the signals not only retain the waveform characteristics of the original signal but also have greater smoothness.

From the experimental results, as shown in Table 5, the data for VMD are lower than those for MA and WT in both RMSE and SD indices. It can be observed that the VMD filtering algorithm achieves higher accuracy and smoothness for the signal. In terms of the SNR index, the data for VMD are higher than those for MA and WT. Since SNR refers to the ratio of useful signal to noise signal in the filtered signal, the signal quality after VMD processing with higher SNR indices is better. In summary, VMD filtering performs best in noise suppression and signal preservation, significantly enhancing the measurement accuracy of vehicle dynamic weighing systems.

Table 5. Signal processing algorithm performance comparison.

Metric	Algorithm	Sensor I (%)	Sensor II (%)
RMSE	VMD vs. MA	↓94.79%	↓93.07%
	VMD vs. WT	↓33.13%	↓94.18%
SD	VMD vs. MA	↓1.96%	↓1.56%
	VMD vs. WT	↓13.76%	↓1.31%
SNR	VMD vs. MA	↑1375.0%	↑855.77%
	VMD vs. WT	↑13.27%	↑17.58%

In the table: ↑: indicates that the VMD algorithm has a higher indicator value than other algorithms (WT or MA). ↓: indicates that the VMD algorithm has a lower indicator value than other algorithms (WT or MA).

The results of this study indicate that applying the VMD filtering algorithm can significantly improve the performance of the vehicle dynamic weighing system. The improved filtering algorithms can provide higher accuracy for vehicle axle weight measurement, assisting transportation authorities in more accurately monitoring overloads and improving road safety. Future research can explore how to fuse data from various sensors to improve the accuracy and robustness of dynamic weighing systems. Multi-source data fusion can effectively reduce the impact of individual sensor errors, providing more accurate weight estimates. Additionally, research can focus on integrating dynamic weighing systems with intelligent transportation systems (ITS), using weighing data for traffic flow analysis, overload detection, and enhancing the intelligence level of traffic management. At the same time, attention should be paid to improving the adaptability and stability of the system under various environmental conditions to ensure reliable operation in complex situations. Dynamic weighing technology can also be used in advanced adaptive vehicle suspension and traction control systems. Both of these systems affect vehicle comfort and safety.

However, VMD makes it difficult to set the optimal parameters without prior knowledge of the signal. Due to the different weights and speeds of driving vehicles, the frequency composition of the collected piezoelectric signals varies, and the number of decomposition layers for each signal and the IMF components to be synthesized are different. The method of trying each decomposition layer one by one is time-consuming in practical use. To solve the difficulty in setting parameters for the VMD filtering algorithm and fully exploit the superiority and availability of the VMD algorithm in signal processing, it is necessary to consider using auxiliary algorithms to determine VMD algorithm parameters in the future.

Author Contributions: Conceptualization, L.X. and A.Y.; methodology, L.X.; software, Z.Z.; validation, L.X.; formal analysis, A.Y. and Z.Z.; investigation, L.X.; resources, T.Z.; data curation, Z.Z.; writing—original draft preparation, L.X.; writing—review and editing, L.X.; visualization, Z.Z.; supervision, T.Z.; project administration, L.X. All authors have read and agreed to the published version of the manuscript.

Funding: This research received no external funding.

Data Availability Statement: The original contributions presented in the study are included in the article; further inquiries can be directed to the corresponding authors.

Conflicts of Interest: The authors declare no conflicts of interest.

References

1. Carr, B.W.J.; Rizenbergs, R.L. Development of an Electronic Means of Weighing Vehicles in Motion. *Ky. Transp. Cent. Res. Rep.* **1971**, 1147. [CrossRef]
2. Li, P.Y.; Li, X.L. Study of Intelligent Measurement for Vehicle Dynamic Weighing. *Chin. J. Sens. Actuators* **2017**, *30*, 899–903. [CrossRef]
3. Kim, S.; Lee, J.; Park, M.S.; Jo, B.W. Vehicle Signal Analysis Using Artificial Neural Networks for a Bridge Weigh-in-Motion System. *Sensors* **2009**, *9*, 7943–7956. [CrossRef] [PubMed]
4. Sinha, A.; Chorzepa, M.G.; Yang, J.J.; Kim, S.H.S.; Durham, S. Deep-Learning-Based Temporal Prediction for Mitigating Dynamic Inconsistency in Vehicular Live Loads on Roads and Bridges. *Infrastructures* **2022**, *7*, 150. [CrossRef]

5. Zhao, S.; Yang, J.; Tang, Z.; Li, Q.; Xing, Z. Methodological Study on the Influence of Truck Driving State on the Accuracy of Weigh-in-Motion System. *Information* **2022**, *13*, 130. [CrossRef]
6. Xie, M.F.; Zhang, P.; Wang, K.D.; Lei, H.M. Research on Attitude Compensated Algorithm for Shipborne Dynamic Weighing. *Phys. Scr.* **2023**, *98*, 115032. [CrossRef]
7. He, Z.J.; Li, Q.; Chu, M.Y.; Liu, G. Dynamic Weighing Algorithm for Dairy Cows Based on Time Domain Features and Error Compensation. *Comput. Electron. Agric.* **2023**, *212*, 108077. [CrossRef]
8. Liu, Y.F.; Niu, Y.G.; Zhang, J.Y. Signal Processing Method for Dynamic Weighing Based on Wavelet Transform. *Ind. Mine Autom.* **2014**, *40*, 13–16. [CrossRef]
9. Cheng, L.; Zhang, H.; Li, Q. Design of a Capacitive Flexible Weighing Sensor for Vehicle WIM System. *Sensors* **2007**, *7*, 1530–1544. [CrossRef]
10. Lan, Q.S.; Ren, X.L.; Li, Y.; Li, Y.X. Synchronous Acquisition System Vehicle Dynamic Weighing. *Integr. Circuits Embed. Syst.* **2018**, *18*, 83–87.
11. Liang, M.; Zhang, Y.; Jiao, Y.; Wang, J.; Su, L.; Yao, Z. Novel Weigh-in-Motion Pavement Sensor Based on Self-Sensing Nanocomposites for Vehicle Load Identification: Development, Performance Testing, and Validation. *Sensors* **2023**, *23*, 4758. [CrossRef] [PubMed]
12. Wang, Y.; Wang, Z.J. Common digital filtering algorithms. *China Metrol.* **2012**, *3*, 99–100. [CrossRef]
13. Deng, L.; LING, T.Y.; He, W.; Kong, X. Refined Tire Model for Analysis of Highway Vehicle-bridge. *China J. Highw. Transp.* **2022**, *35*, 108–116. [CrossRef]
14. Huang, T.; Gao, Q.H.; Liu, Z.H.; Wang, D. Driving Dynamic Characteristics of Multi-Axle Special Vehicles in Shortage of Tires. *J. Shanghai Jiao Tong Univ.* **2023**, *57*, 335–344. [CrossRef]
15. Yang, D.; Deng, G.Q.; Chang, F.S. Design of Non-Stop and Whole Vehicle Weighing System. *Control Eng. China* **2015**, *22*, 1114–1117. [CrossRef]
16. Chen, J. Research on multi-channel data acquisition system for vehicle dynamic weighing. *Xi'an Univ. Technol.* **2022**. [CrossRef]
17. Wang, J.J.; Liu, X.Y. Dynamic weighing technology (WIM) research. *Weigh. Instrum.* **2019**, *48*, 19–24.
18. Hao, X.X.; Niu, Y.G.; Ha, Z.X.; Cai, X.L. Vehicle Dynamic Weighing Algorithm Based on Wavelet and BP Neural Network. *Instrum. Tech. Sens.* **2017**, *8*, 110–113+121.
19. Zhao, Z.; Liu, G.; Wang, Y.; Peng, J.; Qiao, X.; Zhong, J. Research on Dynamic Measurement Method of Flow Rate in Tea Processing. *Sensors* **2022**, *22*, 4294. [CrossRef]
20. Li, D. Design and Implementation of Dynamic Weighing System Based on LabVIEW. *North Univ. China* **2023**. [CrossRef]
21. Zhou, Z.; Cai, P.; Xu, J.; Chen, R. Application of Empirical Mode Decomposition (EMD) in Weigh-in-Motion of Vehicles. *China Mech. Eng.* **2005**, *20*, 1813–1816.
22. Chen, B.; Zhao, H.; Príncipe, J.C.; Liu, X. Maximum correntropy Kalman filter. *Automatic* **2017**, *76*, 70–77. [CrossRef]
23. Du, C.D. Theoretical Analysis of Low-Frequency Dynamic Load and Research on the Algorithm for Weighing Accuracy Improvement. *J. Highw. Transp. Res. Dev. (Engl. Ed.)* **2018**, *12*, 105–110. [CrossRef]
24. Ali, G.; Navid, H.; David, H.; Steve, V.; Win, V.D.B. Performance Assessment of Discrete Wavelet Transform for De-Noising of FBG Sensors Signals Embedded in Asphalt Pavement. *Opt. Fiber Technol.* **2024**, *82*, 103596. [CrossRef]
25. Yin, S.X.; Duan, Y.B.; Liu, Y.F. Variational Mode Decomposition Filtering Combining Mutual Information and Its Application. *J. Jilin Univ. (Inf. Sci. Ed.)* **2019**, *3*, 260. [CrossRef]
26. Chen, X.Y.; Ma, Z.H.; Zhang, H.B.; Qin, G. Research on Vehicle Dynamic Weighing Signal Based on Inertial Sensor. *Autom. Instrum.* **2023**, *38*, 58–62. [CrossRef]
27. Yin, Z.; Wang, X.; Su, X.; Shen, Y.; Xiao, D.; Zhao, H. A Switched Ultra-Local Model-Free Predictive Controller for PMSMs. *IEEE Trans. Power Electron.* 2024, 1–4, *Early Access*. [CrossRef]
28. Lorenzen, S.R.; Riedel, H.; Rupp, M.M.; Schmeiser, L.; Berthold, H.; Firus, A.; Schneider, J. Virtual Axle Detector Based on Analysis of Bridge Acceleration Measurements by Fully Convolutional Network. *Sensors* **2022**, *22*, 8963. [CrossRef] [PubMed]
29. Zhu, Y.; Sekiya, H.; Okatani, T.; Yoshida, I.; Hirano, S. Acceleration-Based Deep Learning Method for Vehicle Monitoring. *IEEE Sens. J.* **2021**, *21*, 17154–17161. [CrossRef]
30. Mohammed, Y.M.; Uddin, N. Acceleration-based bridge weigh-in-motion. *Bridge Struct.* **2018**, *14*, 131–138. [CrossRef]
31. Azam, S.E.; Rageh, A.; Linzell, D. Damage detection in structural systems utilizing artificial neural networks and proper orthogonal decomposition. *Struct. Control. Health Monit.* **2019**, *26*, 2288. [CrossRef]
32. Yang, B.; Lai, Z.C.; YANG, X.X. Research on dynamic weighing algorithm based on CEEMD -GRU model. China Meas. *Test* **2023**, *49*, 108–114. [CrossRef]
33. Dragomiretskiy, K.; Zosso, D. Variational Mode Decomposition. *IEEE Trans. Signal Process.* **2014**, *62*, 531–544. [CrossRef]
34. Zhang, J. The K Value Determination Method of VMD in Signal Decomposition. *J. Lanzhou Univ. Arts Sci. (Nat. Sci.)* **2023**, *49*, 108–114. [CrossRef]